Effective single-particle description of single and multiple processes in $p^{\pm}$ + Ne collisions

T. Kirchner, H. J. Lüdde, and R. M. Dreizler
Institut für Theoretische Physik, Universität Frankfurt, Robert-Mayer-Straße 8, D-60054 Frankfurt am Main, Germany
(Received 21 May 1999; published 14 December 1999)

Single and multiple transitions in $p^{\pm}$ + Ne collisions are discussed within an effective single-particle picture relying on an accurate description of the target ground state in terms of the *optimized potential method*. We show that in the case of proton scattering total cross sections for capture and ionization can be extracted over a broad range of impact energies from the single-particle solutions obtained with the *basis generator method.* In particular, we analyze the role of dynamical screening effects in multiple ionization and propose a simple model for their inclusion in the case of antiproton scattering.

PACS number(s): 34.50.Fa, 34.70.+e

I. INTRODUCTION

Total cross sections (TCS) for ionization and charge transfer in ion-atom collisions have been measured for a large variety of atomic targets, but have so far only been partially analyzed with the aid of quantum theoretical calculations. More specifically, the existing quantal results are mainly restricted to one and two active electron problems, whereas the current understanding of scattering systems with a larger number of electrons is based on classical [1] and statistical [2] models as well as various (semi-)empirical scaling laws (see, e.g., Refs. [3,4]). More sophisticated treatments are relatively rare and mostly restricted to specific physical situations as electron capture in slow collisions, inner-shell processes, or ionization in the perturbative region.

At low projectile velocities, where the coupling to the continuum can be neglected, basis expansion methods in terms of the dominant many-electron molecular states have been used to calculate capture cross sections in collisions between protons and several atomic targets [5]. For higher collision energies the theoretical descriptions commonly start from an effective single-particle picture, since explicit many-electron calculations with inclusion of ionization channels are in general beyond present capabilities. Usually, it is assumed in addition that the many-electron target as well as the projectile, if it carries electrons into the collision, can be described by frozen ground-state potentials during the interaction. In spite of this simplification the solution of the resulting single-particle equations for each initially occupied orbital is a demanding task, in particular if ionization and electron transfer are competing reaction channels. Thus, the validity of the single-particle description with frozen potentials has not been investigated systematically.

In fact, theoretical results for inner-shell processes and outer-shell ionization rely largely on perturbative approaches such as the distorted wave methods [6], which are only applicable at sufficienctly high collision energies and for sufficiently low projectile charges. Only a few nonperturbative calculations for the transitions of the inner [7] and the outer [8] electrons have been reported in the literature.

In recent work [9,10] we have investigated the validity of the single-particle description with a frozen atomic target potential in greater detail and from a more general point of view based on time-dependent density-functional theory (TDDFT) [11]. The basic theorems of TDDFT ensure the existence of an exact mapping between the interacting many-electron problem and an effective single-particle (Kohn-Sham) description, in which a multiplicative effective potential accounts for all electron-electron interaction effects. The basic quantity in this scheme is the one-particle density, which in principle determines all observables of interest and in particular the effective potential in the time-dependent Kohn-Sham equations. The frozen-potential approximation involves the assumption that the variation of the effective potential due to the response of the density in the presence of the projectile can be neglected.

For bare ion impact on neon and argon atoms we have demonstrated that TCS for net electron loss and ionization, which correspond to the average number of ejected electrons, are properly described over a broad range of impact energies as long as the frozen target potential accurately accounts for electronic exchange effects. A multiplicative potential with this property can be obtained from the *optimized potential method* (OPM), which provides the exact exchange-only limit of the exchange-correlation functional of density-functional theory [12]. By contrast, approximate treatments of exchange effects relying on the homogeneous electron gas model in terms of the *local-density approximation* (LDA) or the widely used Hartree-Fock-Slater (HFS) potentials can cause substantial errors. These conclusions were drawn from the results of two different methods for the solution of the single-particle equations with OPM, LDA, and HFS potentials, namely the *continuum distorted wave with eikonal initial state* (CDW-EIS) approximation and the nonperturbative *basis generator method* (BGM) introduced recently [13,14].

Remarkably, our study showed, that it is more important to account for static exchange effects accurately than to include a time-dependent effective potential in the single-particle equations in order to obtain reliable results for the net cross sections. This indicates that recent calculations with the time-dependent version of the LDA for electron capture in slow Ar^{8+} + Ar collisions have to be interpreted with some caution [15].

In this paper we investigate the range of validity and the limitations of the frozen-potential approximation for the collision systems $p^{\pm}$ + Ne in closer detail. For the case of proton impact (Sec. II) we examine the decomposition of the electron loss in its parts capture and ionization contributions

over a broad range of collision energies and calculate cross sections, where the final charge states of projectile and target are determined. This provides a more stringent test of the approximations involved than the net cross sections presented previously [9]. For the case of antiproton impact (Sec. III) we suggest a simple model for an approximate inclusion of response effects and show that the TCS obtained for multiple ionization at low and intermediate impact energies strongly deviate from the results with the frozen potential reported in Ref. [10].

Throughout the paper, we use the exchange-only OPM potential of the neon ground state [12] and solve the single-particle equations with the BGM. For a detailed discussion of the approach the reader is referred to Ref. [10].

In the BGM, the solutions of the single-particle equations are expanded in terms of a basis that dynamically adapts to the collision process under investigation. It is this feature that enables a proper representation of the propagated orbitals — including their overlap with the continuum — within a *finite* set of functions. This strategy has been compared with conventional coupled-channel methods in Ref. [16].

In Ref. [14], we showed that to a good approximation a basis with the desired property is constructed according to

$$\chi_\nu^\mu(\boldsymbol{r},t)=[W_P(\boldsymbol{r},t)]^\mu\varphi_\nu^0(\boldsymbol{r}), \tag{1}$$

where $\{\varphi_\nu^0(\boldsymbol{r}),\nu=1,\ldots,V\}$ denotes a set of bound eigenfunctions of the target system and W_P is the regularized potential of the projectile, whose motion is described by a classical straight line trajectory. The basis set used in the present calculations includes the $KLMN$ states of the neon atom and BGM states $\{\chi_\nu^\mu(\boldsymbol{r},t),\nu=1,\ldots,V,\mu=1,\ldots,M=8\}$, whose population after the collision can be interpreted as electron loss. As has been discussed in Ref. [13], the states of higher order in μ are essential for the representation of the two-center geometry of the collision system.

We extract transition probabilities for capture by explicit projection of the BGM solutions onto traveling projectile states and calculate the single-particle probabilities for ionization by subtraction of single capture from single electron loss. Net electron loss, capture, and ionization are obtained by summation of the respective single-particle probabilities, whereas we use shell-specific binomial and trinomial formulas to calculate multiple transitions [17]. Alternatively, the effects of the Pauli blocking in the final states can be included if the evaluation of the multiple transition observables is based on the formalism of inclusive probabilities [18]. However, we have checked that this does not lead to strong modifications of the results in the present case. In particular, the multiple ionization is not influenced, because the large density of accessible continuum states prevents Pauli blocking from being effective.

II. RESULTS FOR PROTON-NEON COLLISIONS

As stated above, net electron loss in $p^+ + \mathrm{Ne}$ collisions can be precisely calculated if the OPM potential is used for the description of the target potential [9]. In this section, we show that the BGM representation of the single-particle solutions also allows a reliable separation into ionization and capture into the ground state and into excited states of the projectile over a broad range of impact energies (Sec. II A). Moreover, we present results for multiple electron loss, ionization, and capture as well as TCS for the production of one or two holes in specific subshells and analyze the range of validity of the single-particle description with the atomic OPM potential by comparison of our results with experimental data (Sec. II B and II C).

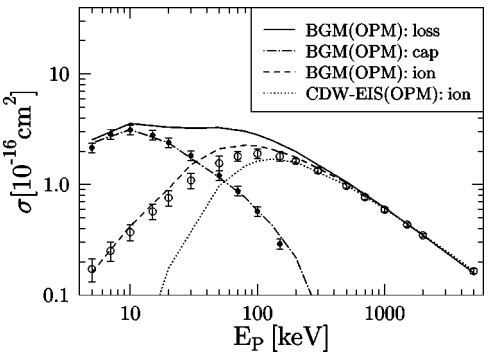

FIG. 1. TCS for net electron loss, ionization (ion), and capture (cap) as a function of impact energy for $p^+ + \mathrm{Ne}$ collisions. Theory: BGM(OPM), present calculation; CDW-EIS(OPM), [9]. Experiment: full circles, capture [23]; open circles, ionization [25].

A. Net electron capture and ionization

Figure 1 shows results for net electron loss, capture, and ionization as a function of the projectile energy obtained from BGM calculations with the OPM potential. The calculated net ionization TCS are within the experimental error bars for collision energies higher than 200 keV. In this region, where the projectile is faster than typical orbital velocities of neon L-shell electrons, the assumption of a frozen atomic potential is reasonable because the distribution of electrons in space does not change considerably during the collision. Moreover, the net ionization is well described at low energies, where single-electron transitions strongly dominate (cf. Sec. II B). This implies, that the behavior of a single active electron does not depend crucially on the response of the system.

At intermediate energies, the experimental data are slightly overestimated. In this region, where multiple processes are more likely to occur, one can expect that the deviation is due to the response effects, which are not included in the frozen-potential approximation. It is obvious that a time-dependent effective potential will reduce the ionization because the target becomes more attractive as ionization sets in.

In addition to the BGM results for net ionization, TCS obtained in the CDW-EIS approximation with the same OPM potential [9] are included in the figure. The results of both methods coincide at energies in the MeV range. This demonstrates that our BGM calculations approach the high-energy limit of perturbation theory. On the other hand, the TCS obtained from the CDW-EIS model differ from the BGM results for projectile energies E_P below 500 keV and

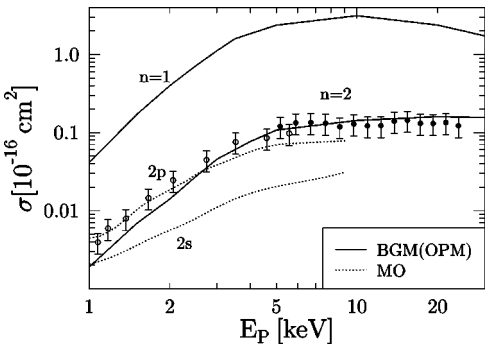

FIG. 2. TCS for capture into specific shells as a function of impact energy for $p^+ + \mathrm{Ne}$ collisions. Theory: BGM(OPM), present calculation; MO, molecular-state calculation for capture into H($2s$) and H($2p$), [21]. Experiment: open circles, capture into H($2p$) [20]; full circles, capture into H($n=2$) obtained from a combination of cross sections for H($2p$) [20] and H($2s$) [21].

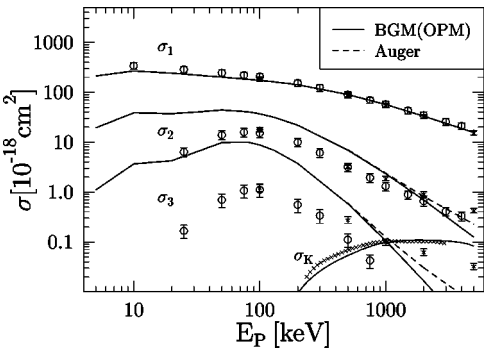

FIG. 3. TCS for q-fold electron loss σ_q and K-hole production σ_K as a function of impact energy for $p^+ + \mathrm{Ne}$ collisions. Theory: BGM(OPM), present calculation; Auger: q-fold loss corrected for Auger processes subsequent to K-hole production. Experiment: q-fold electron loss, open circles [26]; stars, [27]; K-hole production, crosses [19].

underestimate the experimental data for $E_P \leqslant 100$ keV. This clearly demonstrates the limited range of validity of the CDW-EIS model, whereas the BGM is not restricted to a specific energy region.

Moreover, the net electron capture can be described accurately by the BGM in the entire energy range shown. The frozen-potential approximation does not lead to errors, since capture by protons is almost exclusively a single-particle process and the formation of H^- ions is rather unlikely [19]. For the calculation of the net capture TCS the population of the KLM shells of the hydrogenic projectile after the collision have been taken into account. Capture to the ground state strongly dominates, since transitions from the neon L shell ($\varepsilon^{\mathrm{OPM}}_{\mathrm{Ne}(2p)} = -851$ mHartree) to excited hydrogenic states require a larger energy transfer. This is illustrated in Fig. 2, where the TCS for capture to the K and L shells are shown separately. For projectile energies $E_P \geqslant 3$ keV our results for the capture into the L shell agree well with the experimental data taken from [20,21] and thus indicate that the BGM representation is capable of describing not only the dominant but also the weak transition channels. However, we have not separated the L-shell cross sections into the subshell contributions H($2s$) and H($2p$) because this would require the propagation of the solutions to large internuclear distances due to the Stark mixing of degenerate states with the same magnetic quantum number.

Since the experimental data for the H($2s$) channel reported in [21] are restricted to projectile energies $E_P \geqslant 5$ keV, we only show the previously measured cross sections for capture into H($2p$) [20] for the lower energies. They fall off more flatly than our BGM results for total capture into the L shell, which are approximately parallel to the TCS for the dominant capture into the K shell. This behavior indicates that capture to excited states is a two-step process in this region with the ground-state charge-exchange channel as an intermediate state. Since we are not aware of any experimental data for this dominant channel below $E_P = 5$ keV, we cannot give a precise explanation for the discrepancies of the calculated L-shell capture. We conjecture that the quasiadiabatic relaxation of the electronic cloud in the two-center potential of target and projectile nuclei leads to modified couplings between the relevant intermediate states, which cannot be described with a frozen atomic target potential.

B. Multiple-electron transitions

More detailed information about the scattering system can be extracted from the analysis of the final charge-state distributions of projectile and target. First, we consider TCS for multiple electron loss, which corresponds to measurements where only the final charge state of the target is determined. Figure 3 shows corresponding results of our calculations in comparison with different experimental data sets. The agreement is good for one-electron loss, as expected from the discussion of the preceding section, but for two- and three-electron loss deviations occur, which can be attributed to different effects in different energy regions.

At high energies, K-shell ionization with subsequent Auger processes may contribute to the multiple ionization TCS. The figure shows that the direct production of K holes is adequately described by our calculation. The additional Auger processes can be taken into account by a straightforward modification of the binomial formula for the q-fold loss if one assumes that the Auger process occurs independent of the scattering event if a hole in the K shell is produced. Corresponding results are included in the figure (dashed lines). They differ from the TCS of the original calculation in the high-energy region and clearly lead to a better agreement with the experimental data for the two-electron loss. The calculated three-electron loss shows a similar tendency, but no definite conclusion can be drawn for this channel, since the two experimental data sets available are in conflict at high energies.

At lower energies, the K shell is passive and q-fold loss is exclusively due to direct loss from the neon L shell. In this region, the experimental data are overestimated by our results. This can be attributed to response effects, since the projectile velocity is comparably slow and the electrons can adapt to the perturbation of the atomic ground state. Due to the screening of the projectile and the unscreening of the

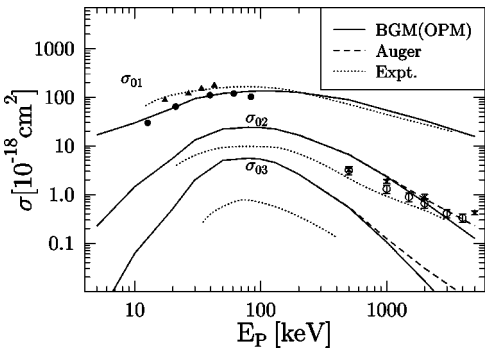

FIG. 4. TCS for single (σ_{01}), double (σ_{02}), and triple (σ_{03}) ionization as a function of impact energy for $p^+ + \mathrm{Ne}$ collisions. Theory: as in Fig. 3. Experiment: dotted lines [19]; triangles [28]; full circles [22]; open circles, q-fold loss [26]; stars, q-fold loss [27].

target nucleus the q-fold loss will be lowered by inclusion of these effects.

Charge-state correlated TCS are shown in Figs. 4 and 5. Again, at intermediate energies multiple processes are overestimated due to response effects. On the other hand, the figures also show that different experiments do not coincide and thus make an unambigious interpretation difficult. For the single ionization channel at low energies (Fig. 4), our calculations support the measurements of Ref. [22]. As the frozen-potential approximation is well justified for one-electron processes pure capture without additional ionization should also be described reliably by our model (Fig. 5). However, the experimental data of Ref. [19] decrease more rapidly than the calculated TCS at energies $E_P \geqslant 100$ keV. This behavior is also in contradiction to the net capture data of Ref. [23] (note that net capture is physically dominated by pure capture). Our calculations clearly favor the results of Ref. [23].

The same problem occurs for the transfer-ionization channels because their slopes at high energies are determined by the rapidly decreasing capture channel. Thus, if the one-electron capture behaves more like the data of Ref. [23], the transfer-ionization data included in Fig. 5 are not reliable.

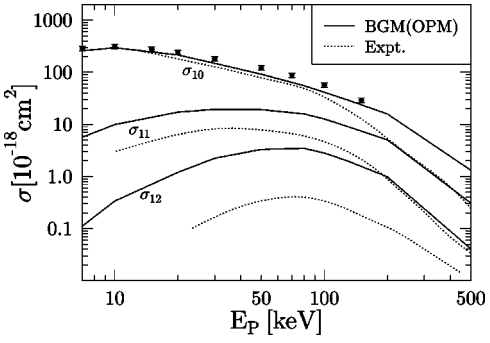

FIG. 5. TCS for pure capture (σ_{10}) and capture with additional ionization of one (σ_{11}) and two (σ_{12}) electrons as a function of impact energy for $p^+ + \mathrm{Ne}$ collisions. Theory: BGM(OPM), present calculation. Experiment: dotted lines [19]; full circles, net capture [23].

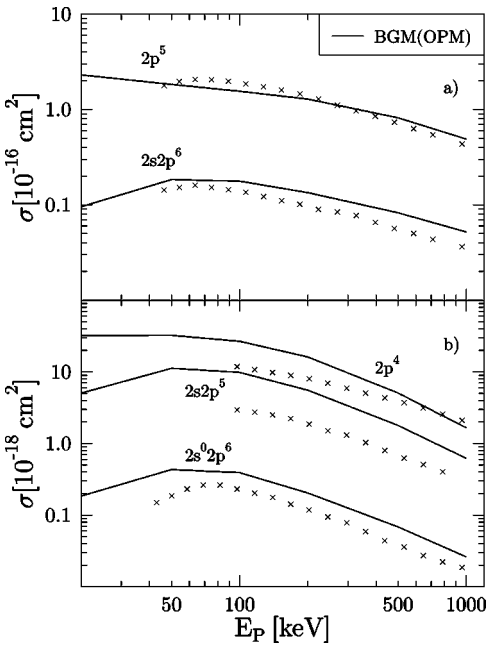

FIG. 6. TCS for $2s$ and $2p$ one (a) and two (b) hole production as a function of impact energy for $p^+ + \mathrm{Ne}$ collisions. The final configurations in the target are indicated in the figure. Theory: BGM(OPM), present calculation. Experiment: crosses [24].

This could — at least partly — explain the deviations with respect to our results in the high-energy region.

C. Subshell-hole production

In addition to inclusive TCS, the ionization from specific subshells has been determined with the aid of photon spectroscopy [24]. Figure 6(a) shows the TCS for the production of a single hole in the target. As before, the corresponding particle-hole probabilities have been calculated by use of shell-specific binomial formulas, since the Pauli blocking does not influence the results significantly. Remarkably, our results for the production of a hole in the L_2 subshell are in better agreement with experiment than those for the production of a hole in the L_1 subshell. Since both processes are one-electron transitions, response effects should be of minor importance and cannot be blamed for the different behavior. Thus, we are led to the conclusion that the L_1-subshell ionization reveals the role of correlation effects which are not included in the orbital picture used.

This interpretation is confirmed by the corresponding results for the production of two holes in definite subshells [Fig. 6(b)]. For the dominant two-particle process, the ionization of two electrons from the L_2 subshell, the deviations between theory and experiment can be attributed to response effects, since the discrepancies are clearly energy dependent and decrease with increasing energy as expected from the justification of the frozen-potential approximation at high energies. The double ionization from the L_1 subshell, however, shows the same behavior as the single ionization from this subshell. In fact, the theoretical results deviate from the experimental data approximately by the same factor in both cases. This is a strong indication that the discrepancies have

the same origin, possibly related to the description of the initial state and its physical interpretation within the orbital picture. The results for the simultaneous removal of one $2s$ and one $2p$ electron seem to reflect both correlation and response effects.

III. RESULTS FOR ANTIPROTON-NEON COLLISIONS

In a recent publication [10] we showed that the frozen-potential approximation leads to monotonically increasing multiple ionization TCS in $p^- + \mathrm{Ne}$ collisions at low-impact energies. In this model the original Ne($2p$) electrons are unbound near the united atom limit instead of approaching the formation of a stable F^- ion. The stability of the corresponding quasimolecule is reached only if one allows for the relaxation of the electronic cloud in the two-center potential of both nuclei.

In order to remedy this flaw, we propose a simple model that accounts for the electronic adaptation in the antiproton-field in a global manner. The important property which has to be incorporated is the increasing target potential in the course of the scattering process due to the reduced screening as ionization sets in. On the other hand, the calculational efforts should not be increased by a determination of an effective potential as a functional of the time-dependent density. Instead, we use a simple ansatz, assuming that the effective potential v_{ee} due to the electron-electron interaction changes uniformly during the collision

$$v_{ee}([n];\boldsymbol{r},t) \approx \left(1 - \frac{P_{\mathrm{net}}^{\mathrm{loss}}(t)}{N}\right) v_{ee}^{\mathrm{OPM}}([n_0];r). \qquad (2)$$

Here, N denotes the number of electrons and $v_{ee}^{\mathrm{OPM}}([n_0];r)$ the atomic ground-state potential. The net electron loss $P_{\mathrm{net}}^{\mathrm{loss}}$, which equals the net ionization in the case of antiproton impact, is the time-dependent information that enters into this ansatz as a measure for the reduction of the mutual screening of the electrons. We have evaluated this quantity in each time step of the propagation of the system in order to use it as input for the time-dependent potential. According to Eq. (2) v_{ee} is reduced by one unit if one electron is removed, and thus vanishes if the target is completely ionized ($P_{\mathrm{net}}^{\mathrm{loss}} = N$). Obviously, the interaction between electrons in the continuum is neglected completely, but this is expected to be of minor importance as long as we are only interested in *total* ionization yields.

Figure 7 shows our results for net, single, double, and triple ionization of neon by antiprotons as obtained with and without the inclusion of the time-dependent part of the effective potential. For energies higher than 200 keV the two sets of calculations deviate only slightly from each other for all channels. In this region the probabilities for electron loss are small and extend over a considerable range of impact parameters. Thus, the response of the potential does not affect the solutions considerably.

In the low-energy region, however, the response effects become more apparent and change the results as could be expected from the preceding discussion. Single ionization is only affected slightly, but multiple ionization is considerably reduced. The deviations of our results from the experimental data for the single ionization at intermediate energies cannot be understood in terms of response effects and remain unexplained. From our point of view it seems more likely that the experiment is in error in this region although the error bars are rather small. It would be of interest if this scattering

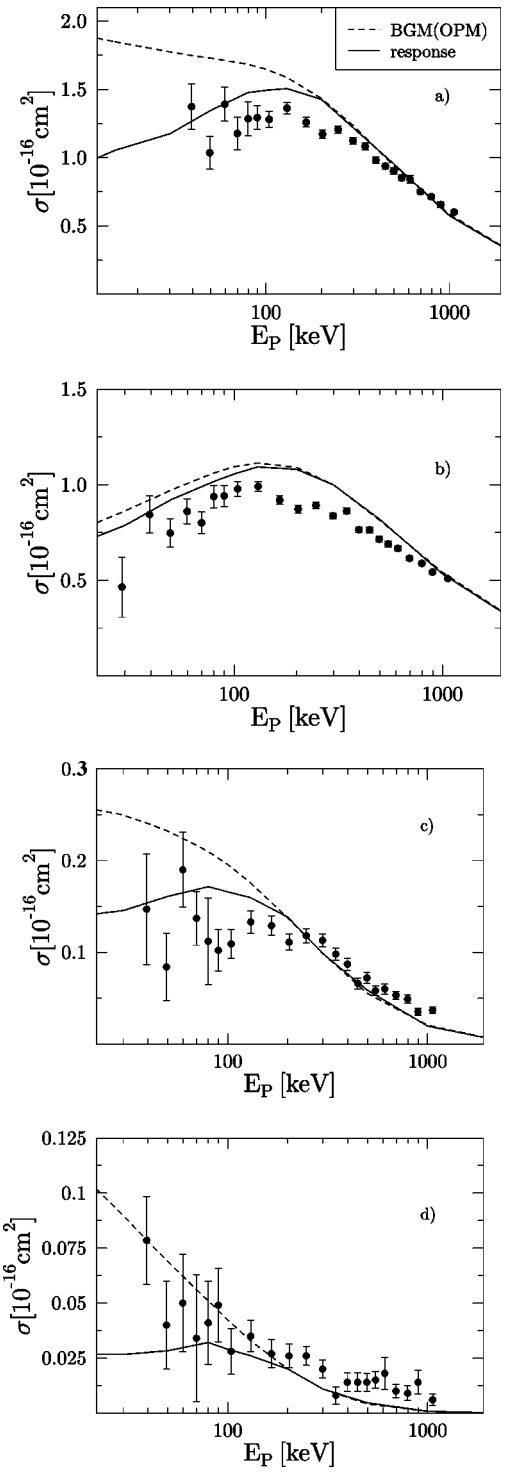

FIG. 7. TCS for net and q-fold ionization as a function of impact energy for $p^- + \mathrm{Ne}$ collisions; (a) net ionization, (b) $q=1$, (c) $q=2$, (d) $q=3$. Theory: present calculation with (full lines) and without (broken lines) response. Experiment: full circles [29].

system could be reexamined experimentally and investigated further in the low-energy region in order to check the reliability of our model on a more quantitative level. At present, we can only conclude that the simple model is able to describe the main effect of the electronic response qualitatively, since it leads to a reduction of the multiple ionization at low and intermediate energies.

IV. CONCLUDING REMARKS

The results of the present study for $p^{\pm}+\mathrm{Ne}$ collisions provide a rather consistent picture for the validity and the limitations of the effective single-particle description with a frozen atomic target potential. An important prerequisite for this discussion is the accurate solution of the time-dependent single-particle equations for all initially occupied orbitals over a broad range of impact energies. Our results clearly demonstrate that the BGM is an adequate tool for this task. The method allows a reliable separation of electron loss into capture and ionization as well as a simultaneous description of the transitions of the strongly bound *K*-shell electrons and the more weakly bound *L*-shell electrons.

With regard to the single-particle description of the many-electron scattering systems we reiterate our main observations.

(1) Net electron loss, ionization, and capture are mainly determined by the target ground-state potential over a broad range of impact energies and are accurately described if static exchange effects are included properly.

(2) In contrast to the dominant single-electron transitions, multiple processes at low and intermediate impact energies are influenced by response effects. For the case of antiproton impact we have shown that these effects can be included on a qualitative level via a simple model.

(3) The electron loss from specific subshells of the target may reveal the limitations of the physical interpretation of the single-particle approach. For the removal of L_1-subshell electrons we have found discrepancies of our results to the experimental data, which cannot be explained by response effects.

A major topic of future work is a more detailed investigation of response effects and their (approximate) inclusion in the description. The simple model proposed for the case of antiproton impact may serve as a starting point for a discussion of response effects in multiple ionization on a qualitative or semiquantitative level. We plan to exploit it further as a first step to a more accurate inclusion of these effects in terms of a truly density-dependent effective potential.

ACKNOWLEDGMENTS

This work was supported in part by the Collaborative Research Grant No. 972997 of the NATO International Scientific Exchange Program. We thank Dr. E. Engel for making his OPM atomic structure calculations available to us.

[1] M. Horbatsch, J. Phys. B **25**, 3797 (1992); R.E. Olson, J. Ullrich, and H. Schmidt-Böcking, *ibid.* **20**, L809 (1987); R. E. Olson, in *Electronic and Atomic Collisions*, edited by H. B. Gilbody, W. R. Newell, F. H. Read, and A. C. H. Smith (Elsevier, Amsterdam, 1988), pp. 271–285.

[2] N.M. Kabachnik, V.N. Kondratyev, Z. Roller-Lutz, and H.O. Lutz, Phys. Rev. A **56**, 2848 (1997).

[3] R. K. Janev, L. P. Presnyakov, and V. P. Shevelko, *Physics of Highly Charged Ions*, Springer Series in Electrophysics Vol. 13 (Springer, Berlin, 1985).

[4] S.H. Be, T. Tonuma, H. Kumagai, H. Shibata, M. Kase, T. Kambara, I. Kohno, and H. Tawara, J. Phys. B **19**, 1771 (1986).

[5] M. Kimura, J.P. Gu, G. Hirsch, and J. Buenker, Phys. Rev. A **55**, 2778 (1997).

[6] P.D. Fainstein, V.H. Ponce, and R.D. Rivarola, J. Phys. B **22**, 1207 (1989); M. McCartney and D.S.F. Crothers, *ibid.* **26**, 4561 (1993); L. Gulyás, P.D. Fainstein, and A. Salin, *ibid.* **28**, 245 (1995).

[7] W. Fritsch and C.D. Lin, Phys. Rev. A **31**, 1164 (1985); A. Toepfer, A. Henne, H.J. Lüdde, M. Horbatsch, and R.M. Dreizler, Phys. Lett. A **126**, 11 (1987); T.G. Winter, Phys. Rev. A **48**, 3706 (1993).

[8] H.J. Lüdde, M. Horbatsch, A. Henne, and R.M. Dreizler, Phys. Lett. A **145**, 173 (1990); B. Hamre, J.P. Hansen, and L. Kocbach, J. Phys. B **32**, L127 (1999).

[9] T. Kirchner, L. Gulyás, H.J. Lüdde, A. Henne, E. Engel, and R.M. Dreizler, Phys. Rev. Lett. **79**, 1658 (1997).

[10] T. Kirchner, L. Gulyás, H.J. Lüdde, E. Engel, and R.M. Dreizler, Phys. Rev. A **58**, 2063 (1998).

[11] E. K. U. Gross, J. F. Dobson, and M. Petersilka, in *Topics in Current Chemistry*, edited by R. F. Nalewajski (Springer, Heidelberg, 1996), Vol. 181, p. 81; C.A. Ullrich and E.K.U. Gross, Comments At. Mol. Phys. **33**, 211 (1997).

[12] E. Engel and S.H. Vosko, Phys. Rev. A **47**, 2800 (1993).

[13] H.J. Lüdde, A. Henne, T. Kirchner, and R.M. Dreizler, J. Phys. B **29**, 4423 (1996).

[14] O.J. Kroneisen, H.J. Lüdde, T. Kirchner, and R.M. Dreizler, J. Phys. A **32**, 2141 (1999).

[15] R. Nagano, K. Yabana, T. Tazawa, und Y. Abe, J. Phys. B **32**, L65 (1999).

[16] T. Kirchner, H.J. Lüdde, O.J. Kroneisen, and R.M. Dreizler, Nucl. Instrum. Methods Phys. Res. B **154**, 46 (1999).

[17] T. Kirchner, H.J. Lüdde, and R.M. Dreizler, Phys. Scr. **T80**, 416 (1999).

[18] H.J. Lüdde and R.M. Dreizler, J. Phys. B **18**, 107 (1985); P. Kürpick, H.J. Lüdde, W.D. Sepp, and B. Fricke, Z. Phys. D: At., Mol. Clusters **25**, 17 (1992).

[19] R.D. DuBois and S.T. Manson, Phys. Rev. A **35**, 2007 (1987).

[20] R. Hippler, W. Harbich, H. Madeheim, H. Kleinpoppen, and H.-O. Lutz, Phys. Rev. A **35**, 3139 (1987).

[21] G.G. Tepehan, B. Siegmann, H. Madeheim, R. Hippler, and M. Kimura, J. Phys. B **27**, 5527 (1994).

[22] R.D. DuBois, Phys. Rev. Lett. **52**, 2348 (1984).

[23] M.E. Rudd, R.D. DuBois, L.H. Toburen, C.A. Ratcliffe, and T.V. Goffe, Phys. Rev. A **28**, 3244 (1983).
[24] M. Eckhardt and K.-H. Schartner, Z. Phys. A **312**, 321 (1983).
[25] M.E. Rudd, Y.-K. Kim, D.H. Madison, and J.W. Gallagher, Rev. Mod. Phys. **57**, 965 (1985).
[26] R.D. DuBois, L.H. Toburen, and M.E. Rudd, Phys. Rev. A **29**, 70 (1984).
[27] L.H. Andersen, P. Hvelplund, H. Knudsen, S.P. Møller, A.H. Sørensen, K. Elsener, K.-G. Rensfelt, and E. Uggerhøj, Phys. Rev. A **36**, 3612 (1987).
[28] V.V. Afrosimov, Yu.A. Mamaev, M.N. Panov, and N.V. Federenko, Zh. Tekh. Fiz. **39**, 159 (1969) [Sov. Phys. Tech. Phys. **14**, 109 (1969)].
[29] K. Paludan, H. Bluhme, H. Knudsen, U. Mikkelsen, S.P. Møller, E. Uggerhøj, and E. Morenzoni, J. Phys. B **30**, 3951 (1997).